Broadband Measurement of Absorption Cross-Section of the Human Body in a Reverberation Chamber

Melia, G. C. R. M.; Robinson, M. P.; Flintoft, I. D.; Marvin, A. C. & Dawson, J. F

Published in IEEE Transaction on Electromagnetic Compatibility, vol. 55, no. 6 , 1043-1050 , 2013, March 20. 2013.

Accepted for publication Jan 2013

DOI: 10.1109/TEMC.2013.2248735

URL: http://ieeexplore.ieee.org/xpl/articleDetails.jsp?arnumber=6482610

PAPER IDENTIFICATION NUMBER TEMC-249-2012

Broadband Measurement of Absorption Cross-Section of the Human Body in a Reverberation Chamber

Gregory C.R. Melia, Martin P. Robinson, Ian D. Flintoft, *Member, IEEE*, Andrew C. Marvin, *Fellow, IEEE*, John F. Dawson, *Member, IEEE*

***Abstract*—We present broadband reverberation chamber measurements of the absorption cross section (ACS) of the human body averaged over all directions of incidence and angles of polarization. This frequency-dependent parameter characterizes the interactions between the body and the enclosures of reverberant environments such as aircraft cabins, and is therefore important for the determination of the overall Q-factor and hence the field strength illuminating equipment inside such enclosures. It also correlates directly with the electromagnetic exposure of occupants of reverberant environments. The average absorption cross section of nine subjects was measured at frequencies over the range 1-8.5 GHz. For a 75 kg male the ACS varied between 0.18 and 0.45 square meters over this range. ACS also correlated with body surface area for the subjects tested. The results agree well with computational electromagnetic simulations, but are obtained much more rapidly. We have used the obtained values of absorption cross section to estimate the effect of passengers on the Q-factor of a typical airliner cabin.**

***Index Terms*—reverberation chamber, absorption cross-section, specific absorption rate, aerospace biophysics.**

I. Introduction

COUPLING of electromagnetic fields within vehicles such as aircraft is important for wireless communications and in determining interference to onboard electronic systems [1]. In this paper we investigate the effect of human bodies on those fields.

In the aerospace industry, the increasing complexity of electronic systems is driving up the cost of testing for electromagnetic compatibility (EMC), prompting an increased reliance on simulation for at least the earlier stages of aircraft design. To develop accurate models, the bodies of passengers and crew need to be taken into account [2].

Aircraft cabins, and also other enclosures such as train carriages, buses and elevators (lifts), are generally fabricated from conducting sheet materials, and thus behave like resonant cavities. At gigahertz frequencies, these enclosures are electrically large and will support many cavity resonances. In this overmoded regime, full-wave simulation of the internal electromagnetic (EM) fields is unfeasible, and a statistical power-balance model is more appropriate [3, 4].

The most important parameter affecting the behaviour of the fields is the average Q-factor of the resonances. A high Q will lead to internal 'hot spots' of enhanced field strength, but power losses through windows, currents in walls and attenuation by absorbing materials will lower the Q-factor, thus reducing the electric and magnetic fields, and increasing the propagation losses. Body tissues at microwave frequencies are lossy dielectrics and their effect on average Q-factor is significant.

Power absorption in bodies can be easily combined with other losses, such as in the passenger seats in an airliner [5]. The absorption effect applies not only in aircraft [6, 7] but also in other confined spaces such as tunnels and mines [8].

In this work we describe the power losses within each body in terms of its absorption cross section (ACS), which is averaged over all angles of incidence and polarization, in order to be applicable to overmoded reverberant environments. Following a review of measurements and calculations of ACS in the literature, we present measurements of ACS, performed in a mode-stirred reverberation chamber. We present results for nine subjects, describe how their ACS varies with frequency, investigate its correlation with body mass and surface area, and thus evaluate the effects of passengers loading a passenger aircraft cabin.

II. Absorption Cross Section (ACS)

The ACS is the ratio of absorbed power, P_{abs}, to incident power density, S_{inc}, and has the dimensions of area:

$$\sigma_{\mathrm{a}} = \frac{P_{\mathrm{abs}}}{S_{\mathrm{inc}}}. \tag{1}$$

Human ACS will generally be less than the actual surface area of the body, or even than its projected or 'silhouette' area, because a substantial portion of the incident power is reflected from or transmitted through the body.

ACS varies with frequency, direction of the incident wave, and polarization, and is closely related to the whole body specific absorption rate (WBSAR), an important parameter in EM dosimetry:

$$\sigma_{\mathrm{a}} = \mathrm{WBSAR}\ \frac{m}{S_{\mathrm{inc}}}, \tag{2}$$

where m is body mass. Hence knowledge of the ACS allows the exposure to a reverberant EM field to be assessed.

It is important to distinguish between the *average* ACS

Manuscript received August 31, 2012. The research leading to these results has received funding from the European Community's Seventh Framework Programme [FP7/2007-2013] under grant agreement n° 205294.

The Authors are with the Department of Electronics, University of York, York, YO10 5DD, UK. (e-mail: martin.robinson@york.ac.uk; ian.flintoft@york.ac.uk; andy.marvin@york.ac.uk; john.dawson@york.ac.uk)

$\langle \sigma_a \rangle$, which is what we are interested in for a reverberant environment, and the ACS in a *particular direction* σ_a. In calculations of WBSAR, researchers often need the worst case, i.e. the highest absorbed power. Note also that literature sources sometimes refer to 'average WBSAR' meaning averaged over all parts of the body, rather than over multiple directions and polarizations of the incident wave.

A. Measurements of ACS

Published data on the average ACS of the human body at microwave frequencies are scarce. In our previous work [9] we estimated it at 910 MHz from the changes to the Q of a screened room (with no mechanical stirring) containing up to nine people, and obtained a value of 0.25 m^2.

Hurst and Ellingson [6] state that average ACS for a typical person is about 0.4 m^2 at 2.1 GHz, varying very slowly with frequency; however no experimental evidence is presented to support this assertion.

Andersen et al. [7] estimated average ACS from the effects of people on the reverberation time of a mock-up of an aircraft cabin, getting a value of 0.33 m^2. This was averaged over a very broad frequency range of 3 to 8 GHz. Narrowband measurements, also obtained from the reverberation time but in an office environment, are presented by Bamba et al. [10]. They found that the average ACS was 0.34 m^2 at 2.3GHz and 0.36 m^2 at 3 GHz.

ACS can also be found from measurements in a reverberation chamber [11] (see also Section III.A). Harima [12] obtained the WBSAR of a male 70.6 kg in mass and 1.7 m high. From this data the subject's average ACS decreased with frequency from 0.33 m^2 at 1 GHz to 0.11 m^2 at 4 GHz.

The above values of ACS are approximately 10-20% of the total body surface area of an adult: reference data published by the International Commission on Radiological Protection [13] gives this as 1.6 m^2 for a female and 1.8 m^2 for a male.

Interestingly, the ACS can also be measured for sound waves. Conti et al. [14] measured the average ACS of adults in an *acoustic* reverberant chamber as 0.1 to 0.2 m^2. The absorption mechanism here is clearly different, sound waves being absorbed mostly by clothes and EM waves being attenuated by high-water-content tissues, but the ACS is of a similar order of magnitude.

B. Calculation of ACS

Exposure to EM waves can be simulated with computational EM codes such as transmission line matrix (TLM) or finite-difference time-domain (FDTD). Many detailed human body models (phantoms) have been created in order to calculate WBSAR, as this is a key parameter for international guidelines limiting human exposure [15]. If the source of the simulated radiation is in the far field:

$$\sigma_a = \frac{P_{abs}}{E^2/\eta_0} = \text{WBSAR}\ \frac{m\eta_0}{E^2}, \qquad (3)$$

where E is the RMS amplitude of the incident electric field and η_0 is the impedance of free space, approximately 377 Ω.

So we can get the ACS from the WBSAR using the incident electric field and the mass of the phantom, but only for a single direction of incidence and polarization. Usually the phantom is standing, and the wave vertically polarized and incident from the front, to give the worst-case exposure, i.e. the highest WBSAR. The WBSAR in this orientation initially increases with frequency, shows a broad resonance between 10 and 100 MHz (the peak varying with body shape) and then decreases much more slowly between 200 MHz and 2.4 GHz [16]. Substituting the WBSAR for male or female phantoms at 1 GHz into (3) gives the *maximum* ACS at low microwave frequencies as 0.48 m^2 for males and 0.46 m^2 for females.

These high-resolution models require a lot of computing power and time, so repeating the simulation for sufficient numbers of different directions of incidence and polarization to gain an accurate average is time consuming. Moglie et al. did this with FDTD in the VHF band (25 to 200 MHz), and found that the peak absorption at 75 MHz persisted even after averaging [17]. However they reported that it took 200 processors 18 hours to calculate a single frequency point.

Conil et al. performed FDTD simulations at 2.1 GHz of a 105 kg male [18]. With the subject standing, they varied the azimuth angle of the incident wave to include all horizontal directions, but only varied the angle of elevation by ±20°. This excludes waves coming from directly above or below, which would probably give the lowest WBSAR.

Uusitupa et al calculated WBSAR from FDTD simulations at five frequencies from 300 MHz to 5 GHz, and over a range of angles, with 30° steps in azimuth and elevation [19]. Details of how we weighted these values to obtain an average ACS are given in Section IV.B. However it is straightforward to calculate upper and lower limits on averaged ACS, by applying (3) to the maximum and minimum WBSAR over different orientations. Results for their 72.24 kg male phantom are listed in Table I, along with the measured values described in Section II.A.

Passengers and crew on an aircraft are often seated rather than standing. Uusitupa [19] also calculated WBSAR for six different phantom postures at the frequencies in Table I, for two polarizations, but with just one direction of incidence (horizontal, from the front). The WBSAR, and hence ACS, was 8 to 22% lower for 'sitting' than for 'standing.'

TABLE I
AVERAGE ACS OF HUMAN BODY FROM 0.9 TO 8 GHZ: LITERATURE VALUES

frequency (GHz)	$\langle \sigma_a \rangle$ (m^2)	measured/ simulated	reference
0.90	0.27-0.51	s	[19]
0.92	0.25	m	[8]
1.0	0.33	m	[11]
2.1	0.21-0.47	s	[19]
2.3	0.28-0.42	m	[9]
2.5	0.20	m	[11]
3.0	0.24-0.43	m	[9]
3.5	0.16-0.37	s	[19]
4.0	0.11	m	[11]
5.0	0.12-0.31	s	[19]
3.0-8.0	0.33	m	[6]

The data in Table I show large uncertainties in ACS or in frequency, indicating a need for more precise measurements. The simulations only used a single body phantom, while for some of the measurements the individual body dimensions are not recorded, hence our interest in also studying how ACS relates to body size and type.

III. Theory

A. Power balance model

As frequency increases the resonant modes of an aircraft cabin or a reverberation chamber become more closely spaced, and eventually a statistical approach to describing their behavior becomes appropriate. According to Hill et al. [4], the various contributions to the average Q-factor of the enclosure can then be combined thus:

$$Q_{\mathrm{av}}^{-1} = Q_1^{-1} + Q_2^{-1} + Q_3^{-1} + Q_4^{-1}, \tag{4}$$

where Q_1 represents losses in the metal walls, Q_2 absorption by lossy dielectrics, Q_3 the effects of apertures (windows) and Q_4 the losses in any measuring antennas.

If there are several absorbers, the contribution of absorber i to the second term in (4) can be found from its average ACS:

$$Q_{2i} = \frac{2\pi V}{\lambda < \sigma_{\mathrm{a}i} >}, \quad Q_2^{-1} = \frac{\lambda}{2\pi V} \sum_i < \sigma_{\mathrm{a}i} >, \tag{5}$$

where V is the cavity volume and λ the wavelength. So if we assume that the average ACS of each person is unaffected by others nearby, we can simply add all their cross-sections, and thus characterize their effect on EM propagation.

In order to apply this approach, it is necessary to determine the frequency above which a statistical multimode environment model is appropriate. The Helmholtz equation was used to calculate the resonant modes in the fuselages (modeled as cuboids, based on the interior cabin dimensions) of an airliner (based on Boeing 747), a small helicopter (based on Bell Jet Ranger) and an executive jet (based on Learjet 85). Fig. 1 shows the mode densities (these were counted using a 50 MHz moving window, which covered enough modes to provide a realistic assessment of the mode count). As can be seen, the airliner exceeds 10 modes/MHz at 150 MHz, while the Jet Ranger achieves this density at nearer 1500 MHz. At 1 GHz, the airliner typically has over 1000 modes within the bandwidth of the resonant modes (f/Q), meaning that many modes are excited at any given frequency and a reverberant cavity is an appropriate model for the aircraft's cabin at this and higher frequencies. At the same frequency, the Bell's cabin supports 5 modes / MHz, so while no Q factor data is available for this aircraft, a Q of 100 (similar to the loaded 747 cabin in Fig. 8) would give a resonance bandwidth of 10MHz, or 50 resonant modes. So all three aircraft can be appropriately modeled as resonant cavities at our frequencies of interest (1 to 8.5GHz).

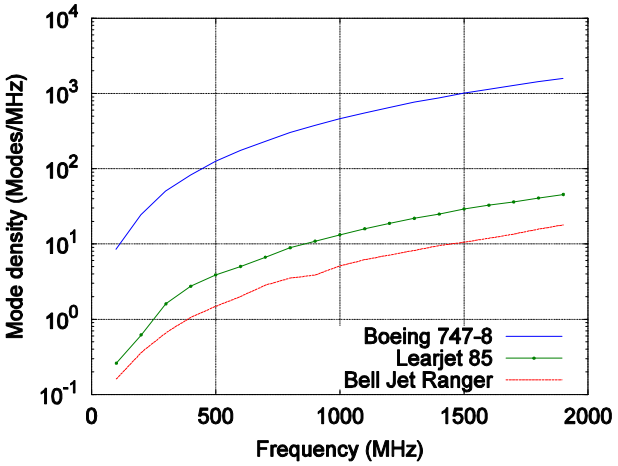

Fig. 1. Resonant mode density in the cabins of three aircraft.

B. ACS in a Reverberation Chamber

In a stirred-mode reverberation chamber a mechanical perturber, such as a rotating paddle, randomizes the internal propagation paths. Average ACS is obtained from the scattering (S) parameters S_{ij}, between two antennas, measured with and without a test object inside the chamber.

Following Carlberg et al. [20] we define a normalized chamber transmission factor, G, as

$$G = \frac{\left\langle |S_{21}|^2 \right\rangle}{(1 - |\langle S_{11} \rangle|^2)(1 - |\langle S_{22} \rangle|^2)}, \tag{6}$$

where angle brackets represent averaging over all n stirrer positions. If we take the ratio of the measured G-factors for 'no object' and 'with object' as $G_r = G_{\mathrm{no}}/G_{\mathrm{wo}}$, the average ACS is given by

$$< \sigma_{\mathrm{a}} > = \frac{\lambda^2}{8\pi}\left(\frac{1}{G_{\mathrm{wo}}} - \frac{1}{G_{\mathrm{no}}}\right) = \frac{\lambda^2}{8\pi\, G_{\mathrm{no}}}(G_{\mathrm{r}} - 1) \cdot \tag{7}$$

and its statistical uncertainty is

$$\frac{\delta < \sigma_{\mathrm{a}} >}{< \sigma_{\mathrm{a}} >} = \frac{\sqrt{2} G_{\mathrm{r}}}{G_{\mathrm{r}} - 1} \frac{\delta G}{G}, \tag{8}$$

TABLE II
PLANE WAVE PENETRATION OF EM WAVES INTO TISSUES (cm)

Frequency (GHz)	Skin	Fat	Muscle
1	3.9	23	4.1
2.5	2.2	11	2.2
5.0	1.1	4.9	0.93
8.5	0.49	2.4	0.43

where

$$\frac{\delta G}{G} = \frac{k}{\sqrt{n}}, \tag{9}$$

and k determines the confidence (68 % for k=1, 95 % k=2) [21].

The above method assumes lossless antennas. If there are ohmic losses, the ACS should be multiplied by the product

of the two antenna radiation efficiencies. [12, 20] It is therefore important to use low loss, broadband antennas to minimize systematic error. In this study we assumed each antenna's radiation efficiency to be 95%, based on ongoing measurements of our own horns and on measured data for similar horn antennas [22].

Further improvement to the uncertainty (at the expense of losing some frequency resolution) is achieved by 'frequency stirring' which means averaging the S-parameters over a narrow band of frequencies as well as over stirrer positions.

C. Absorption in the human body

At microwave frequencies, body tissues are lossy dielectrics. Their complex permittivity is frequency-dependent and can be obtained from parametric models [23]. Standard EM theory then gives the plane wave penetration depth d_p.

Table II shows d_p for the tissues closest to the surface of the body. The value for other soft tissues is similar to that of muscle, while bone is comparable to fat. It is evident that attenuation is high (except in fat at the lower end of our frequency range), so most power absorption will occur near the surface of the body.

Models of the human body, such as the IT'IS Virtual Family [2], typically have a voxel dimension of 2 mm, which allows FDTD simulation up to 15 GHz. To simulate the fuselage of a large airliner such as the Boeing 747 ($V \approx 2500 m^3$) at this resolution would require ~300 GB of RAM. Given that our primary interest is EMC aboard the aircraft rather than dosimetry in the passengers, the precise energy distribution within the body is unimportant: all we need to know is the power absorbed. These voxel models are therefore overly complex for our purposes – a simpler model is needed.

IV. Measurement Technique

A. Reverberation chamber measurements

Measurements were taken in a reverberation chamber with dimensions 4.70m × 3.00m × 2.37m and a lowest usable frequency (LUF) of 200MHz [24], using two double ridged waveguide horn antennas. These were connected to a vector network analyzer through N-type bulkhead connectors in the chamber wall. A full 2-port calibration was performed at the connectors on the antenna ports. Frequency sweeps were made using 1601 points, spaced at approximately 5 MHz intervals from 1 GHz to 8.5 GHz. The network analyzer used a 6 dBm stimulus (keeping the worst-case WBSAR well within exposure guidelines [15]), and 70 kHz IF bandwidth.

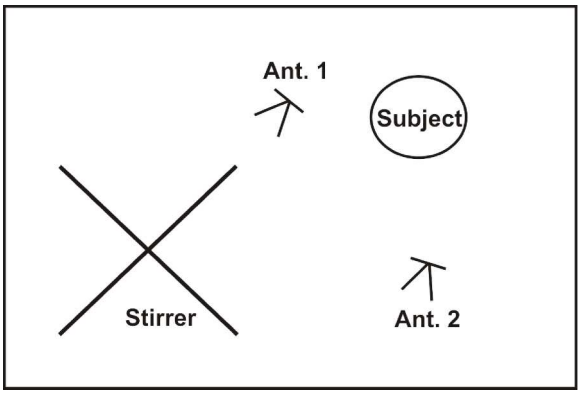

Fig. 2. Diagram of reverberation chamber setup for ACS measurements.

The equipment was arranged in the reverberation chamber as shown in Fig. 2. In order to eliminate direct path, the port 1 antenna was aimed at the stirrer, while the port 2 antenna was pointed at a chamber wall at approximately 45°. This gave a ratio of unstirred to stirred energy in the chamber (K-factor) of typically 0.01, rising to 0.07 at the lowest frequencies in the loaded chamber. In order to eliminate the remaining unstirred energy, during post-processing the S_{21} was vector averaged over all stirrer positions. This average was then subtracted from the S_{21} for each individual position:

$$S_{21}' = S_{21} - \langle S_{21} \rangle \tag{10}$$

The resulting change in S_{21} was as large as 10% at the low end of the frequency range, but within 1% at high frequencies. This is consistent with stirring being more effective at higher frequencies – as is indicated in the previous paragraph, and is shown in Fig. 3, where S_{21} is autocorrelated over stirrer movements – the higher the frequency, the smaller a movement is required to give an independent S_{21}.

Normalized transmission factors were then calculated using (6) and ACS was then calculated using (7). Frequency stirring was applied using a window size of 20 points, i.e. 100 MHz. This window size was chosen as an acceptable compromise, providing additional stirring to the existing mechanical stirring, without being so large as to obscure any resonances or other features of the measurement. As such, 100MHz can be taken to be the frequency resolution of these results.

B. Validation

Our measurement technique was validated in two ways: by measurement of a test object [11], and by comparison to values of human ACS in the literature described above.

The test object was a dielectric sphere filled with water, for which σ_a is the same in all directions and can be obtained analytically from Mie scattering theory [25]. Over the range 1-8.5 GHz its ACS is approximately 0.07 m^2 with a measurement uncertainty of 11 to 13%. The differences between measured and calculated ACS were within this uncertainty.

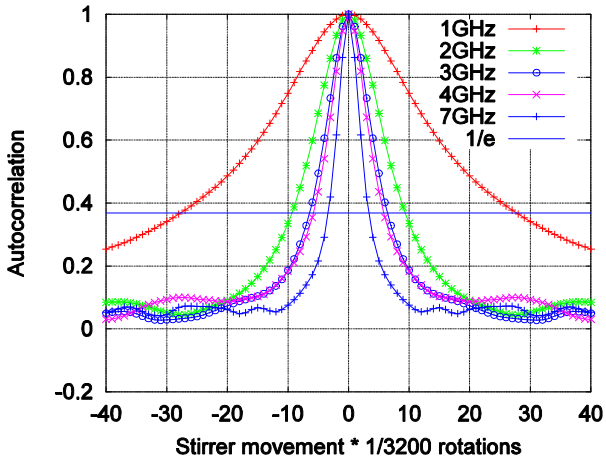

Fig. 3. Autocorrelation of S_{21} over mechanical stirrer movement.

The WBSAR of the Virtual Family (VF) heterogeneous male phantom has been calculated in [18], for plane wave illumination at 11 angles of arrival and 2 polarizations using FDTD simulations. An unweighted average of the ACS from these 22 different illuminations is however biased since the 22 samples are not uniformly distributed with angle of arrival. This bias results in a significant overestimate of the average ACS, since angles of arrival corresponding to the smaller silhouette areas are under-represented. In order to construct an unbiased estimate of the average ACS from these results an ellipsoidal model of the phantom silhouette area was constructed. Regarding the phantom as an ellipsoid with estimated semi-major axes a = 0.10 m, b = 0.20 m and c = 0.89 m the silhouette area for angle of arrival (θ,φ) is [26]

$$S(\theta,\varphi)=\pi\sqrt{(bc\sin\theta\cos\varphi)^2+(ac\sin\theta\sin\varphi)^2+(ab\cos\theta)^2}\,. \quad (11)$$

The true average silhouette area over 4π steradians for the ellipsoidal model is found to be

$$\langle S\rangle_{\text{unbiased}}=\frac{1}{4\pi}\iint_{4\pi}S(\theta,\varphi)\,\mathrm{d}\Omega=0.337\ \mathrm{m}^2\,, \quad (12)$$

whereas the average silhouette area over the i = 1,…,11 angles of arrivals in the FDTD simulations is

$$\langle S\rangle_{\text{biased}}=\frac{1}{11}\sum_{i=1}^{11}S(\theta_i,\varphi_i)\sin\theta_i=0.382\ \mathrm{m}^2\,, \quad (13)$$

indicating an overestimate by a factor of 1.13. The range over angles of arrival of the Uusitupa ACS simulation results at 300, 450, 900, 2100, 3500 and 5000 MHz, together with the biased and estimated unbiased averages are shown in Fig. 6.

C. Human subjects

Nine subjects were recruited locally, after obtaining ethical permission to experiment on volunteers, and selected to give a range of different physical characteristics (Table III).

TABLE III
PHYSICAL PARAMETERS OF MEASURED SUBJECTS

Subject	Gender	height (m)	mass (kg)
1	Male	1.89	101
2	Male	1.81	75.7
3	Female	1.65	84.1
4	Male	1.76	101.5
5	Male	1.75	67.8
6	Female	1.54	38.1
7	Male	1.81	59.3
8	Female	1.72	52.8
9	Male	1.95	112.2

Subjects wore light clothes. Before entering the chamber, they were briefed on the experiment and photographed. We recorded their gender, age, mass and height, a description of their clothing, and the room temperature.

All subjects sat on the same wooden stool inside the chamber, which was registered to markings on the floor, 1.5 m × 1 m from the chamber walls. Subjects were asked to keep their feet on the cross-bar of the stool in order to keep them within the stirred volume of the chamber, i.e. more than 7.5 cm from the floor at 1 GHz and above. They were also asked to remain still as far as possible during the measurement.

Fig. 3 relates to a measurement of the empty chamber, where the stirrer was moved over one complete rotation in 3200 steps. The S_{21} was then autocorrelated over stirrer movement, at several frequencies across the range of interest. At 1GHz, 28 steps were required to produce an independent S_{21} (using a metric of 1/e). This gives 3200/28 = 114 independent stirrer positions in the chamber at 1GHz. For the human subjects, measurements were taken over 100 mechanical stirrer positions in one full rotation. Using fewer than 115 steps meant that all samples were independent over the whole frequency range. This setup gave a total measurement time of approximately 15 minutes, which was felt to be the longest that subjects could be asked to sit still in the chamber. This is the limiting factor on the statistical error in the ACS results.

V. RESULTS

A. Human ACS values

Fig. 5 shows ACS versus frequency for all nine subjects. The uncertainty in ACS for each plot, estimated from (8), is approximately 10-12% [11]. In the 1 to 2 GHz band the higher statistical uncertainty due to the lower number of independent samples available in the chamber limits the ability to resolve the differences in ACS between the subjects.

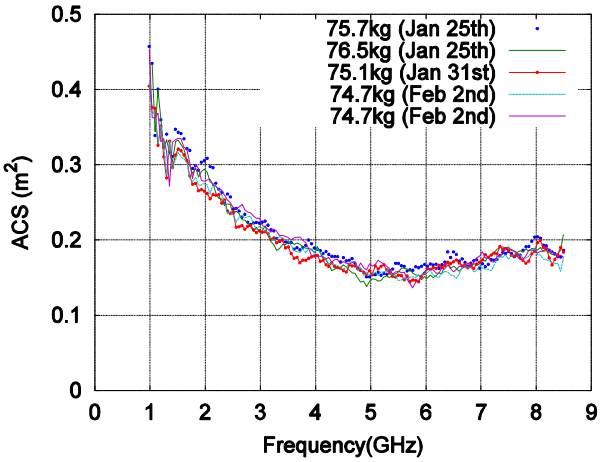

Fig. 4. ACS of one subject measured five times on different days.

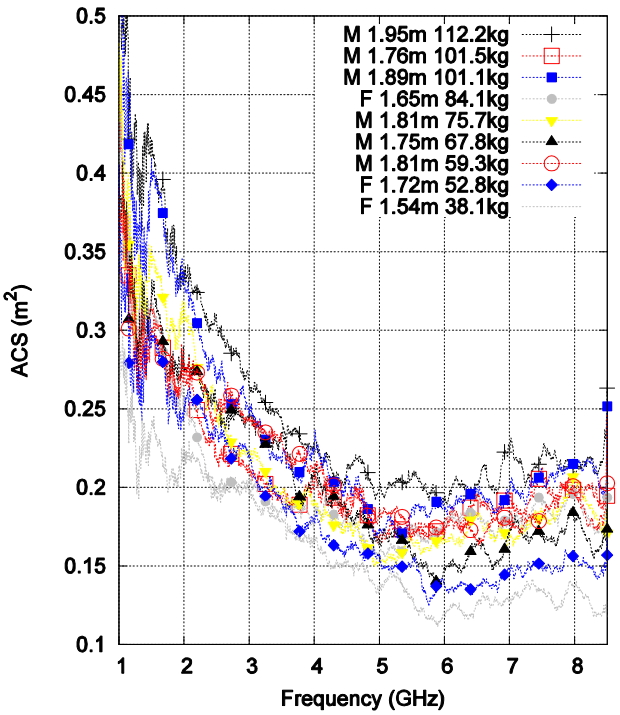

Fig. 5. ACS of nine human subjects measured in the York reverberation chamber.

To investigate the repeatability of our technique, one subject was measured five separate times on different days. These results are shown in Fig. 4 and indicate that the measurement procedure is robust.

These results give ACS values that are slightly low compared to some of those given in the literature. Our subjects' ACS values range from 0.22 to 0.34 m^2 at 2.1 GHz, compared to Hurst and Ellingson's 0.4 m^2. Between 3 and 8 GHz, averaged values vary around 0.2 m^2, as compared to Andersen's 0.33 m^2. Bamba's value of 0.34 m^2 at 2.4 GHz is within our range, although Bamba does not predict the drop in ACS by 3 GHz.

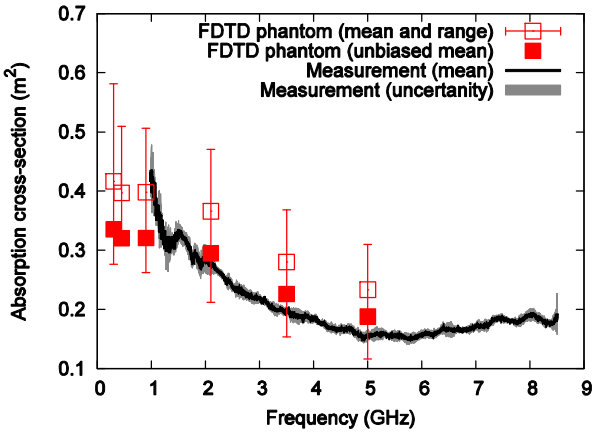

Fig. 6. Measured ACS of a 75.7kg male subject compared to Uusitupa's FDTD simulation of the VF heterogeneous male phantom based on plane wave incidence from 11 directions with two polarisations.

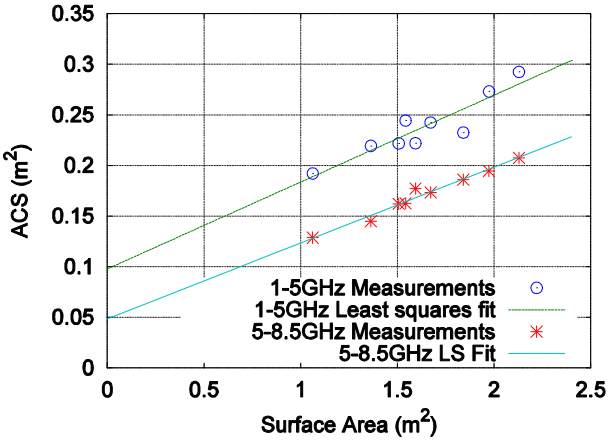

Fig. 7. Correlation of average human ACS with body surface area.

Uusitupa's multi-angle SAR simulation does, however, predict this drop; our measurements are particularly close to the values of Uusitupa once the latter have been unbiased for the limited number of angles of incidence, as described in Section IV B.

Despite the measurement uncertainties, it can be seen from Fig. 5 that average ACS is generally greater for the larger subjects, as might be expected. This relationship is illustrated further in Fig. 7, where the ACS of each subject is averaged over frequency and plotted against body surface area. The body surface area (BSA) in m^2 was estimated from the subject's height, H, in m and mass, m, in kg using the Dubois & Dubois equation (14) [13].

$$\mathrm{BSA} = 0.20247 H^{0.725} + m^{0.425} \quad (14)$$

The ACS to BSA relationship is plotted in two ranges: below 5GHz where the ACS reduces with frequency and above 5GHz where ACS appears to be more frequency independent.

The frequency-averaged ACS correlates with surface area but is not directly proportional to it, rather the proportionality breaks down at low values, so the linear regression fit does not intersect the origin. The correlation is much stronger for the higher frequency range, which is as expected: not

only does the chamber support more resonant modes and thus a higher degree of confidence at these frequencies, the penetration depth of human tissues is also smaller, so that absorption is a surface effect which is predictably well-correlated with surface area. At lower frequencies, EM waves penetrate further into the inner tissue layers and anatomically-dependent internal scattering effects are more significant.

The measurements of ACS shows good agreement with data from the literature. The technique is much faster than computation by TLM or FDTD, giving average ACS at 1601 frequencies in 15 minutes rather than several hours per frequency point. Measurement time could be further reduced by optimizing the sweep time and paddle speed, while taking care that the sweep time is not too short to allow the chamber to reach a steady state at each measured frequency point.

B. Effect of human ACS on an airliner cabin's Q factor

The ACS data was used to calculate the effect of a full complement of passengers on the Q factor of a modern airliner cabin. The Q of an empty Boeing 707 (without seats) was obtained from [27]. The passenger cabin dimensions were then obtained for a 707 and a 747-8, from the respective airport planning manuals [28], and the 747's empty-cabin Q was estimated, based on scaling the wall and window areas using the equations provided in [4]. We added 400 airline seats, with their ACS calculated as in [5]. We then added 400 passengers, based on the averaged ACS of six of the measured subjects: 1, 2, 3, 5, 6 and 8. These six were selected to give three men and three women, and have an average mass of 69.9kg and height of 1.73m, which are both well within the standard deviations of these properties for British adults [29]. The resulting effect on the 747 Q-factor can be seen in Fig. 8, where the addition of the passengers reduces the cabin's Q factor by around 50%.

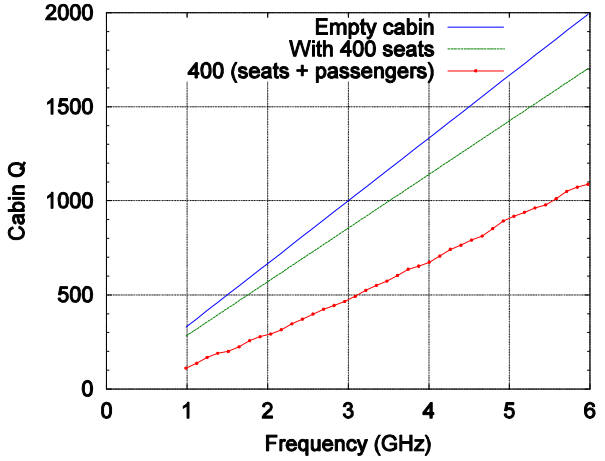

Fig. 8. Estimated effect of 400 passengers on the Q factor of a 747-8 cabin.

VI. Conclusion

Broadband measurements (1 to 8.5 GHz) of the absorption cross section of the human body, averaged over multiple directions of incidence and angles of polarization, in a reverberation chamber have been presented. The ACS of a typical 75 kg subject is around 0.40 m^2 at 1 GHz, falls to a minimum of 0.16 m^2 at about 5 GHz, then rises slightly to 0.18 m^2 at 8.5 GHz. The ACS is found to be correlated with body surface area: larger subjects have greater cross-sections. We have estimated the uncertainties of the measurement as 10-12% and validated it against literature data.

This work enables us to estimate the effect of people on the Q-factors of enclosures, leading to a better understanding of propagation in resonant environments such as aircraft – where they are shown to have a significant effect, halving the Q of a typical airliner's passenger cabin. The ACS of a subject exposed to EM waves is closely related to his or her WBSAR, so this work is also relevant to the field of EM dosimetry.

Future work to improve this method could include taking a larger sample of subjects, to give a better understanding of the correlation of ACS with body dimensions, and hence the effect of a typical population of passengers and crew on the EM environment in aircraft.

Also of interest would be the effect of clothing on ACS, the influence of body posture, and of the total ACS of a person sitting in an airline seat. The slightly lower values of average ACS compared to the FDTD simulations may be because the real subjects were sitting, while the phantom was simulated standing.

We also intend to explore the ACS at higher frequencies: the upper end of the range is only limited by the performance of the network analyzer, cables and antennas.

References

[1] C. De Raffaele, C. J. Debono, and A. Muscat "Modeling electromagnetic interference generated by a WLAN system onboard commercial aircraft" *MELECON 2010 - 15th IEEE Mediterranean Electrotechnical Conference* Valletta, Malta 26-28 April 2010

[2] G.C.R. Melia, M.P. Robinson, and I.D. Flintoft, "Development of a layered broadband model of biological materials for aerospace applications," in *EMC Europe 2011 York*, Sept. 2011, pp. 84 –89.

[3] I. Junqua, J.Parmantier and F. Isaac, "A network formulation of the power-balance method for high-frequency coupling" *Electromagnetics*, vol. 25 pp. 603-622, 2005.

[4] D. Hill, M. Ma, A. Ondrejka, B. Riddle, M. Crawford, and R. Johnk, "Aperture excitation of electrically large, lossy cavities," *IEEE Trans. Electromag. Compat.*, vol. 36, no. 3, pp. 169–178, 1994.

[5] T. Nguyen, "RF loading effects of aircraft seats in an electromagnetic reverberating environment," in *Proc. 18th Digital Avionics Systems Conference*, 1999, vol. 2, pp. 10.B.5–1 – 10.B.5–7.

[6] K. W. Hurst and S. W. Ellingson "Path loss from a transmitter inside an aircraft cabin to an exterior fuselage-mounted antenna" *IEEE Trans. Electromag. Compat.*, vol. 50, no. 3, pp. 504–512, 2008.

[7] J. B. Andersen, K. L. Chee, M. Jacob, G. F. Pedersen and T. Kürner, "Reverberation and absorption in an aircraft cabin with the impact of passengers" *IEEE Trans. Antennas and Propagation*, vol. 60, no. 5, pp. 2472–2480, 2012.

[8] I. Ben Mabrouk, L. Talbi, M. Nedil and K. Hettak "The effect of the human body on MIMO-UWB signal propagation in an underground mine gallery," *J. Electromag. Waves and Applications*, Vol 26 no. 4, pp 560-569, 2012

[9] M. P. Robinson, I. D. Flintoft and G. C. R. Melia "People and planes: development of broadband EMC models of biological materials in aircraft", *General Assembly and Scientific Symposium, 2011 XXXth URSI, Istanbul 13-20 Aug. 2011*

[10] A. Bamba, W. Joseph, J. B. Andersen, E. Tanghe, G. Vermeeren, D. Plets, J. Ø. Nielsen and L. Martens "Experimental assessment of specific absorption rate using room electromagnetics" *IEEE Trans. Electromag. Compat.*, vol. 54, no. 4, pp. 747–757, 2012

[11] G. C. R. Melia, I. D. Flintoft and M. P. Robinson, "Absorption cross section of the human body in a reverberant environment", EMC Europe Conference, Rome, 17th-21st Sept. 2012

[12] K. Harima "Estimation of power absorbed by human body using reverberation chamber", IEEE Symposium on Electromagnetic Compatibility, Pittsburgh, 5th-12th Aug. 2012
[13] International Commission on Radiological Protection 1975, *Report on the Task Group on Reference Man*, ICRP Publication 23, Pergamon, Oxford, p 17
[14] S. G. Conti, P. Roux and D. A. Demer, "Measurements of the total scattering and absorption cross-sections of the human body", *J. Acoust. Soc. Am.* vol. 114, pp. 2357-2357, 2003
[15] ICNIRP, "Guidelines for limiting exposure to time-varying electric, magnetic and electromagnetic fields (up to 300 GHz)," *Health Phys.*, vol. 44, pp. 1630–1639, 1998.
[16] E. Conil, A. Hadjem, F. Lacroux, M. F. Wong and J. Wiart "Variability analysis of SAR from 20 MHz to 2.4 GHz for different adult and child models using finite-difference time-domain" *Phys. Med. Biol.* vol 53 pp 1511–25, 2008
[17] F. Moglie, V. M. Primiani, and A. P. Pastore "Modeling of the human exposure inside a random plane wave field" *Progress In Electromagnetics Research B*, Vol. 29, pp 251-267, 2011
[18] E. Conil, A. Hadjem, A. Gati M.-F. Wong and J. Wiart "Influence of plane-wave incidence angle on whole body and local exposure at 2100 MHz" *IEEE Trans. Electromag. Compat.*, vol. 53, no. 1, pp. 48–52, 2011.
[19] T. Uusitupa, I. Laakso, S. Ilvonen, and K. Nikoskinen, "SAR variation study from 300 to 5000 MHz for 15 voxel models including different postures," *Phys. Med. Biol.*, vol. 55, no. 4, pp. 1157-1176, 2010.
[20] U. Carlberg, P.-S. Kildal, A. Wolfgang, O. Sotoudeh, and C. Orlenius, "Calculated and measured absorption cross sections of lossy objects in reverberation chamber," *IEEE Trans. Electromag. Compat.*, vol. 46, no. 2, pp. 146 – 154, 2004.
[21] J. Kostas and B. Boverie. "Statistical model for a mode-stirred chamber", *IEEE Trans. Electromag. Compat.*, Vol. 33, No. 4, pp. 366–370, November 1991
[22] C.L. Holloway, H.A. Shah, R. Pirkl, W.F. Young, D.A. Hill and J. Ladbury, "A three-antenna technique for determining the total and radiation efficiencies of antennas in reverberation chambers", *IEEE Antennas and Propagation Magazine*, vol. 54, no. 1, pp235-241, Feb. 2012
[23] S. Gabriel, R. W. Lau and C. Gabriel, "The dielectric properties of biological tissues. III. Parametric models for the dielectric spectrum of tissues", *Phys. Med. Biol.* vol. 41, pp 2271-2293, 1996
[24] J. Clegg, A. C. Marvin, J. F. Dawson and S. J. Porter, "Optimization of stirrer designs in a reverberation chamber", *IEEE Trans. Electromag. Compat.*, vol. 47, no. 4, pp824-832, 2005.
[25] O. Pena and U. Pal, "Scattering of electromagnetic radiation by a multilayered sphere", *Computer Phys. Communications* Vol. 180 pp2348-2354, 2009
[26] G. T. Vickers, "The projected areas of ellipsoids and cylinders", *Powder Technology*, Vol. 86, pp. 195-200, 1996.
[27] D.M. Johnson, M.O. Hatfield and M.B. Slocum 1997, "Phase II demonstration test of the electromagnetic reverberation characteristics of a large transport aircraft", Dahlgren Division Naval Surface Warfare Centre, Joint Warfare Applications Department
[28] Boeing Commercial Airliners Division, "Boeing 7X7: Airplane Characteristics for Airport Planning"
[29] K. Sproston and P. Primatesta, "Health survey for England 2003 vol. 2, Risk factors for cardiovascular disease", pp160-162

Gregory C.R. Melia received the M.Eng. degree in Electronic Engineering from the University of York, York, U.K. in 2008. After a time as a youth worker, he returned to York in 2009, since when he has been studying for the Ph.D. degree under the supervision of Dr Martin Robinson. His chief research interest is in bioelectromagnetics.

Martin P. Robinson received the B.A. and M.A. degrees from the University of Cambridge, Cambridge, U.K., in 1986 and 1990, respectively, the M.Sc. degree in medical physics from the University of Aberdeen, Aberdeen, U.K., in 1990, and the Ph.D. degree in dielectric imaging from the University of Bristol, Bristol, U.K., in 1994. He worked for two years with the National Physical Laboratory and for three years with the Bristol Oncology Centre, U.K. In 1993, he joined the University of York, York, U.K., where he is currently a Senior Lecturer in the Department of Electronics. His current research interests include design for electromagnetic compatibility, electromagnetic measurements, and the interaction of electromagnetic radiation with biological tissues.

Ian D. Flintoft (M'00) received B.Sc. and Ph.D. degrees in physics from the University of Manchester, Manchester, U.K., in 1988 and 1994, respectively. Between 1988 and 1994, he was with Philips Research Laboratories, Redhill, U.K., for two years as a Scientist in the Simulation and Signal Processing Group. Since 1996, he has been a Research Fellow in the Physical Layer Research Group, University of York, North Yorkshire, U.K., where his research focuses on the immunity of digital systems, electromagnetic compatibility in complex and distributed systems, and electromagnetic compatibility aspects of telecommunication systems. His research interests include computational electromagnetics, material measurements, and bioelectromagnetics.

Andrew C. Marvin (M'85–SM'06-F'11) is Technical Director of York EMC Services Ltd and Professor of Applied Electromagnetics, leading the Physical Layer Research Group in the University of York's Department of Electronics. He received his BEng, MEng and PhD degrees from the University of Sheffield between 1972 and 1978. He is a Fellow of the Royal Academy of Engineering. He is an elected Member of the IEEE EMC Society Board of Directors (2010-2012), Vice-Chairman of the IEEE Std-299 Working Group on Shielding Effectiveness Measurement, an Associate Editor of IEEE Trans EMC and a Faculty Member of the IEEE EMCS Global University. His main research interests are EMC measurement techniques and shielding.

John F. Dawson (M'90) received the B.Sc. and D.Phil. degrees in electronics from the University of York, York, U.K., in 1982 and 1989, respectively.
He is currently a Senior Lecturer and a member of the Physical Layer Research Group at the University of York. His current research interests include numerical electromagnetic modeling, electromagnetic compatibility (EMC) prediction for circuits and systems, EMC test environments, optimization techniques for EMC design, and propagation in vehicles and buildings.